

D.R. OLIINYCHENKO,^{1,2} V.V. SAGUN,¹ A.I. IVANYTSKYI,¹ K.A. BUGAEV¹¹ Bogolyubov Institute for Theoretical Physics, Nat. Acad. of Scs. of Ukraine
(14b, Metrolohichna Str., Kyiv 03680, Ukraine; e-mail: dimafopf@gmail.com,
v_sagun@ukr.net, a_iv_@ukr.net, bugaev@th.physik.uni-frankfurt.de)² FIAS, Goethe-University, Frankfurt
(1, Ruth-Moufang Str., Frankfurt am Main 60438, Germany)**SEPARATE CHEMICAL FREEZE-OUT
OF STRANGE PARTICLES WITH CONSERVATION LAWS**

PACS 25.75.-q, 25.75.Nq

The Hadron Resonance Gas Model with two freeze-outs connected by the conservation laws is considered. We are arguing that the chemical freeze-out of strange hadrons should occur earlier than the chemical freeze-out of non-strange hadrons. The hadron multiplicities measured in the heavy ion collisions for the center-of-mass energy range 2.7–200 GeV are described well by such a model. Based on a success of such an approach, a radical way to improve the Hadron Resonance Gas Model performance is suggested. Thus, we suggest to identify the hadronic reactions that freeze-out noticeably earlier or later than most of the others reactions (for different collision energies they may be different) and to consider a separate freeze-out for them.

Keywords: Hadron Resonance Gas Model with the multicomponent hard-core repulsion, hadron multiplicity ratios, chemical freeze-out, Strangeness Horn, strange hadrons.

1. Introduction

The hadronic multiplicities measured in heavy ion collisions and in the collisions of elementary particles are traditionally described by the Hadron Resonance Gas Model (HRGM) [1–5]. It is based on the assumption that the fireballs produced in such collisions reach a full thermal equilibrium. Using this assumption, it is possible to describe the hadronic multiplicities registered in experiment with the help of two parameters: temperature T and baryo-chemical potential μ_B . The parameters T and μ_B obtained from the fit of multiplicities for various collision energies correspond to the stage of chemical freeze-out. Its physical meaning is that the inelastic collisions at this stage cease simultaneously for all sorts of particles. However, in such a simple form, the concept of chemical freeze-out works well for the hadrons, which consists of the u and d (anti)quarks, while the strange hadrons demonstrate a deviation from the chemical equilibrium. At the same time, the hydrodynamic simulations (see, e.g., the review [6]) rather successfully reproduce the transverse momentum spectra of strange particles. This is an old problem of the thermal approach. In order to account for the observed deviation of strange particles from the com-

plete chemical equilibrium, the additional parameter γ_s , the strangeness suppression factor, was suggested [7] long ago. Although the concept of strangeness suppression proved to be important both in the collisions of elementary particles [4] and in nucleus-nucleus collisions [4, 8], the problem of its justification remains unsolved. Thus, up to now, it is unclear which is the main physical reason responsible for the chemical non-equilibrium of strange hadrons.

Moreover, it is well known [2] that the fit of hadron multiplicities with the strangeness suppression factor γ_s improves the quality of a data description, but still the fit seldom attains a good quality, especially at low collision energies. This is clearly seen from the center-of-mass energy behavior of two most prominent ratios that involve the lightest strange meson, i.e. K^+/π^+ , and the lightest strange baryon, i.e. Λ/π^- , which, so far, cannot be successfully reproduced [2, 4, 8] by the traditional versions of the HRGM. In addition, the ratios involving the multistrange hyperons Ξ and Ω exhibit the apparent failure of the γ_s fit at the center-of-mass energies $\sqrt{S_{NN}} = 8.76, 12.3, \text{ and } 17.3$ GeV [2]. Since the γ_s fit does not improve their description sizably, we conclude that there should exist a different reason for the apparent deviation of strange hadrons from the chemical equilibrium. Hence, the concept of chemical freeze-out requires a further development.

© D.R. OLIINYCHENKO, V.V. SAGUN,
A.I. IVANYTSKYI, K.A. BUGAEV, 2014

ISSN 2071-0194. Ukr. J. Phys. 2014. Vol. 59, No. 11

Recently, an alternative concept of chemical freeze-out of strange hadrons was suggested [9]. Instead of a simultaneous chemical freeze-out for all hadrons, two different chemical freeze-outs were suggested: one for particles containing strange charge, even hidden, (we refer to it as the strangeness freeze-out, i.e. SFO) and another one (FO) for all other hadrons, which contains only u and d (anti)quarks. A partial justification for the SFO hypothesis is given in [10–12], where the early chemical and kinetic FO of Ω hyperons and J/ψ and ϕ mesons is discussed for the energies at and above the highest SPS energy. In this article, we further develop and refine the SFO concept of Ref. [9] and present a more coherent and detailed picture of two freeze-outs together with new arguments which allow us to better justify and to improve the performance of the HRGM.

The paper is organized as follows. In the next section, we discuss the concept of chemical freeze-out in some details and give the arguments that, in a meson-dominated hadronic medium, the SFO should occur earlier than the FO. Section 3 is devoted to the description of the HRGM with the multicomponent hard-core repulsion. The results are presented in Section 4, and Section 5 contains our conclusions and suggestions.

2. Framework of the Thermal Model

In 1950 in his pioneering paper [13], E. Fermi suggested to use the statistical model to find the outcome of high energy nucleon-nucleon collisions. Since there were produced from 10 to 30 hadrons in such reactions, they were named as the processes of multihadron production. According to E. Fermi, the large number of particles in the final state of these processes naturally suggests to apply the methods of statistical mechanics. The next crucial step suggested by E. Fermi was a justification of the thermal equilibrium assumption due to the strong interaction between particles. A few years later, L. D. Landau suggested to apply the relativistic hydrodynamics to the reactions of multihadron production [14], because the applicability conditions of relativistic hydrodynamics are basically the same as for the full (local) thermal equilibrium, if the strong discontinuities are absent.

Since that time, the assumption of thermal equilibrium at some stage of the multihadron production reactions was tested experimentally both in the nucleon-nucleon collisions and in the collisions of

heavy ions. In other words, the outcome of such reactions was compared to the results of statistical models. The coincidence between the statistical models predictions and the experimental results appeared to be good both for the nucleon-nucleon collisions and for the heavy ion collisions at the energy range starting from the center-of-mass energy $\sqrt{S_{NN}} = 2$ GeV per nucleon in the fixed target experiments performed at the Brookhaven AGS up to the center-of-mass energy $\sqrt{S_{NN}} = 2.76$ TeV achieved at the Large Hadron Collider [2, 15]. It was even suggested that, for the high energy electron-positron collisions, the statistical model can also describe the hadron multiplicities [3]. However, a more thorough analysis [16] showed later on that even within a rather sophisticated canonical ensemble consideration, the discrepancy between theory and experiment is rather large with $\chi^2/\text{dof} > 5$.

Let us now consider, in some details, a particular set of models used to describe hadron multiplicities in nucleon or heavy ion collisions, that are known as the HRGM [1–5, 8, 15]. A common feature of this set of models is the assumption that, at some time moment, there exists a fireball consisting of all possible hadronic states being locally in the thermal and chemical equilibria. The term “chemical equilibrium” means that the rates of forward and backward reactions are equal, i.e., for any hadron species, the rate of its production is equal to the rate of its destruction. The characteristic time of equilibration varies with collision energy, but one can safely say that it lies within the interval of 0.1–10 fm/c [17–19]. This means that one can safely ignore the weak interaction, because its characteristic time is essentially longer. Therefore, the baryon charge B , strange charge S , isospin projection I_3 , charm charge C , and bottom charge are conserved in almost all hadron reactions. Some of the most frequent hadronic reactions read: $\pi\pi \rightarrow \rho \rightarrow \pi\pi$, $\pi K \rightarrow K^* \rightarrow \pi K$, $\pi N \rightarrow \Delta \rightarrow \pi N$. They lead to the thermal equilibration, but do not change the number of particles. Another reactions, such as $\pi N \rightarrow N^* \rightarrow \Delta\pi \rightarrow N\pi\pi$, change the number of particles and lead to the chemical equilibration. Was such a system of all hadron states kept in a finite box of volume V , it would inevitably equilibrate both thermally and chemically at $t \rightarrow \infty$. Let us define the characteristic time of equilibration between the species A and B τ_{AB} as the average time when some typical number of collisions between A

and B occurred. If there are only A and B species in the box, then $\tau_{AB} \sim \frac{1}{n_A n_B \sigma_{AB}}$, where σ_{AB} is the AB reaction cross-section, and $n_A(n_B)$ denote the concentration of species A (B). If one considers a gas of many species in the box out of equilibrium, then the equilibration times will be defined from the system of equations (assuming only the reactions $2 \rightarrow 1$ and $1 \rightarrow 2$):

$$\frac{dN_i}{dt} = \sum_{AB} \frac{N_A N_B v_{AB}^{\text{rel}}}{V} \sigma_{AB \rightarrow i} - \sum_A \frac{N_i N_A v_{Ai}^{\text{rel}}}{V} \sigma_{Ai \rightarrow B} - \sum_{CD} \Gamma_{i \rightarrow CD} N_i, \quad (1)$$

where N_i , N_A , and N_B are the number of hadrons of the corresponding kind, σ denotes the corresponding cross-sections, and Γ is the decay rate. The first term on the right-hand side describes the formation of particles of kind i , the second term stands for the particle destruction of this kind in the $2 \rightarrow 1$ reaction, and the third term stands for the decays of this kind of particles. From these equations, one can see that the larger production cross-section leads to a faster equilibration, while the larger volume leads to a slower equilibration. One can also see that, depending on the cross-sections of production and decay and on the volume, the equilibration times for different species may be different. These equations are, of course, oversimplified, because they do not include the momentum dependencies. If one introduces such dependencies, then one obtains the system of Boltzmann equations, and, hence, Eq. (1) can be regarded as the system of Boltzmann equations averaged over momenta. However, even these oversimplified equations can help to understand the way how a system approaches an equilibrium. For instance, from Eq. (1), one can see that increasing the box volume n times is equivalent to decreasing all the cross-sections by n times. One can also see that, for very large volumes, only the decays will occur.

If the system is expanding, i.e. $V = V(t)$, then there is no guarantee that all particle species will be at the chemical and thermal equilibria at any time. The simplest way to qualitatively characterize an expanding system is to introduce a set of characteristic times: expansion time t_{ex} , thermalization time t_{th} , and chemical equilibration t_{ch} time for different species. It is known that, typically of the reactions

of strongly interacting particles, there is the inequality $t_{\text{ch}} \gg t_{\text{th}}$ [17–19]. It is equivalent to the statement that the cross-sections of reactions, which lead to a chemical equilibration, are much smaller than the cross-sections of reactions, which lead to a thermalization. During the expansion process, the system volume increases, or one can say equivalently that all cross-sections effectively decrease by the same factor. Therefore, the reactions, which lead to a chemical equilibration will cease earlier, than the reactions, which lead to a thermalization, they are called, respectively, as chemical and kinetic freeze-outs. Since the cross-sections of different reactions are not the same, one can say generally about the chemical and kinetic freeze-outs for each particle species.

Typically in vacuum, the reactions involving strange particles have smaller cross-sections than the reactions involving only non-strange particles (charm and bottom are not considered here at all). Then, from our previous consideration, one can conclude that if the cross-sections and the thresholds of hadronic reactions occurring at the late stage of the expansion do not differ from their vacuum values, then the chemical equilibrium for strange particles should be lost earlier. The kinetic freeze-out for strange particles is also going to occur earlier than the kinetic freeze-out of non-strange hadrons, but later than the chemical freeze-out for any hadron species. These conclusions are based on the following hierarchy of the switching-off times of hadronic reactions:

$$\begin{aligned} t_{K\Lambda \rightarrow \Sigma p} &> t_{\pi N \rightarrow N^* \rightarrow \Delta \pi \rightarrow N \pi \pi} \gg \\ &\gg t_{K\pi \rightarrow K^* \rightarrow K \pi} > t_{N\pi \rightarrow \Delta \rightarrow N \pi}. \end{aligned} \quad (2)$$

It is not only cross-sections that influence the freeze-out times. As one can see from Eq. (1), the smaller the concentrations, the lower the rates of reactions are expected. The numbers of strange particles different from kaons are smaller than the number of protons, and this is one more factor that makes slower the reactions of strangeness exchange and leads to the earlier freeze-outs of strange particles. Of course, one should keep in mind that this simplified treatment is valid at low particle densities, if the approximation of binary reactions is reasonable, and if the surrounding medium does not essentially modify the reaction threshold. Therefore, the appearance of the results that contradict the conclusions above should be considered as a signal that the chemical freeze-out

picture based on Eqs. (1) and (2) is not justified, and, hence, one has to seek for another explanation.

Nevertheless, the argumentation above motivates one to consider a separate chemical freeze-out of strange particles in the HRGM. This was done recently in two independent studies [9, 20] and [21]. In [21], three free parameters were taken for FO (temperature, baryon chemical potential, and volume) and three free parameters of the same kind for SFO. The electric charge chemical potential μ_Q was taken from the condition $N_B/N_Q = 2.5$ for both freeze-outs. Species subjected to the SFO were all strange particles and the ϕ -mesons. The strange charge was treated canonically, and the particle multiplicities were fitted. The approach of [9, 20] is quite different. The parameters of FO and SFO were connected by the conservation laws, namely the baryon number conservation, I_3 conservation, and entropy conservation. Both freeze-outs were treated grand canonically, and the ϕ mesons were not subjected to the earlier freeze-out. In addition, in contrast to the oversimplified treatment of the equation of state, the HRGM of [9] includes the width of all hadron resonances and the short-range repulsion, which is taken into account via the excluded volume corrections, while these important features were neglected in [21].

We would like to stress, although being simple and successful in describing the hadronic multiplicities, the approach suggested in [21] violates the above-mentioned conservation laws. Moreover, in such approach, it might happen that not only the entropy conservation is violated, but the entropy may decrease from an earlier freeze-out to the later one. Finally, while the number of fitted multiplicities is rarely exceeding 10 per one collision energy value, having six fitting parameters for each energy value seems to be excessive. Therefore, we outline an alternative model [9] below, which seems to be physically more relevant.

3. Model Formulation

In the simplest version, the HRGM represents the gas of hadrons being in the chemical and thermal equilibria, which is described by the grand canonical partition function. The multiplicity of particles of mass m_i and degeneracy g_i is given by

$$N_i = g_i V \int \frac{d^3 k}{(2\pi)^3} \frac{1}{e^{(\sqrt{m_i^2 + k^2} - \mu)/T} \pm 1}, \quad (3)$$

where the sign $+(-)$ in the equation above stays for the Fermi (Bose) statistics, and μ_i denotes the full chemical potential $\mu_i = \mu_B B_i + \mu_S S_i + \mu_{I_3} I_{3i}$ of particles of sort i , B_i is their baryonic charge, S_i is their strange charge, and I_{3i} denotes their third projection of isospin. The chemical potentials μ_B , μ_S , and μ_{I_3} , which correspond to the conserved charges, can be found from the conservation laws

$$\sum_i N_i B_i = B^{\text{init}}, \quad (4)$$

$$\sum_i N_i S_i = S^{\text{init}}, \quad (5)$$

$$\sum_i N_i I_{3i} = I_3^{\text{init}}. \quad (6)$$

Then the temperature T and the system volume V will be free parameters. One can, however, take T and μ_B as free parameters, and this is a conventional choice. In [22], we argued that, for mid-rapidity, the quantities B^{init} and I_3^{init} are anyway unknown, so one can fit the ratios and have T , μ_B , and μ_{I_3} as the fitting parameters. Using this procedure, one gets the hadron multiplicities that correspond to the full thermal equilibrium. To get the final particle multiplicities, one has to take the decays of hadron resonances into account (see below).

An extension of the HRGM to two freeze-outs is almost obvious in the case of [21], where both non-strange and strange freeze-outs have their own parameters and are by no means connected. In such a case, one considers two separate ideal gases with their own parameters. However, if one follows the way described in [9], then some complications arise. One problem is to properly include the conservation laws, then one has to take the excluded volume into account in a consistent way. By consistency, we mean that the standard thermodynamic identities should be obeyed. One more issue is a change of the entropy between two freeze-outs due to the decays of strange resonances. However, as we argued in [9], the latter is negligible, because the time interval between two freeze-outs is short.

We would like to stress that the excluded volume for all particles remains the same after the SFO. Indeed, not all reactions between the strange and non-strange particles cease, but only those with the strangeness exchange. For instance, the reaction $\pi K \rightarrow \rightarrow K^* \rightarrow \pi K$ survives after the SFO. It keeps the

same excluded volume between pions and kaons, but does not provide the chemical equilibrium for kaons.

After these comments, let us formulate our approach. It is based on the multicomponent formulation of the HRGM [5], which is currently the best at describing the observed hadronic multiplicities. Therefore, it is natural to apply such a formulation to describe both the FO and the SFO. The present HRGM was worked out in [5, 22–28]. The interaction between hadrons is taken into account via the hard-core radii, with the different values for pions R_π , kaons R_K , other mesons R_m , and baryons R_b . The best fit values for such radii ($R_b = 0.2$ fm, $R_m = 0.4$ fm, $R_\pi = 0.1$ fm, and $R_K = 0.38$ fm) were obtained in [5]. The main equations of the model are listed below, but more details of the model can be found in [5, 22].

We consider the Boltzmann gas of N hadron species in a volume V that has the temperature T , baryonic chemical potential μ_B , strange chemical potential μ_S , and chemical potential of the isospin third component μ_{I3} . The system pressure p and the K -th charge density n_i^K ($K \in \{B, S, I3\}$) of the i -th hadron sort are given by the expressions

$$\frac{p}{T} = \sum_{i=1}^N \xi_i, \quad n_i^K = \frac{Q_i^K \xi_i}{1 + \frac{\xi^T \mathcal{B} \xi}{\sum_{j=1}^N \xi_j}}, \quad \xi = \begin{pmatrix} \xi_1 \\ \xi_2 \\ \dots \\ \xi_N \end{pmatrix}, \quad (7)$$

where \mathcal{B} denotes a symmetric matrix of the second virial coefficients with the elements $b_{ij} = \frac{2\pi}{3}(R_i + R_j)^3$, and the variables ξ_i are the solutions of the following system:

$$\xi_i = \phi_i(T) \exp \left[\frac{\mu_i}{T} - \sum_{j=1}^N 2\xi_j b_{ij} + \xi^T \mathcal{B} \xi \left[\sum_{j=1}^N \xi_j \right]^{-1} \right], \quad (8)$$

$$\phi_i(T) = \frac{g_i}{(2\pi)^3} \int \exp \left(-\frac{\sqrt{k^2 + m_i^2}}{T} \right) d^3k. \quad (9)$$

Here, the full chemical potential of the i -th hadron sort is defined as before, $\phi_i(T)$ denotes the thermal particle density of the i -th hadron sort of mass m_i and degeneracy g_i , and ξ^T denotes the row of variables ξ_i .

The width correction is taken into account by averaging all expressions containing the resonance mass

by the Breit–Wigner distribution having a threshold (see, e.g., [1] for more details). The effect of resonance decay $Y \rightarrow X$ with the branching ratio $BR(Y \rightarrow X)$ on the final hadronic multiplicity is taken into account as $n^{\text{fin}}(X) = \sum_Y BR(Y \rightarrow X) n^{\text{th}}(Y)$, where $BR(X \rightarrow X) = 1$ for the sake of convenience. The masses, widths, and strong decay branchings of all hadrons were taken from the particle tables used by the thermodynamic code THERMUS [29].

The SFO is assumed to occur for all strange particles at the temperature T_{SFO} , baryonic chemical potential $\mu_{B_{\text{SFO}}}$, isospin third projection chemical potential $\mu_{I3_{\text{SFO}}}$, and three-dimensional space-time extent (effective volume) of the freeze-out hypersurface V_{SFO} . The FO of hadrons, which are built of the u and d (anti)quarks, is assumed to be described by its own parameters T_{FO} , $\mu_{B_{\text{FO}}}$, $\mu_{I3_{\text{FO}}}$, and V_{FO} . The obtained model parameters for two freeze-outs and their $\sqrt{S_{NN}}$ dependence are shown in Figs. 1–2. Equations (7)–(9) for FO and SFO remain the same as for a simultaneous FO of all particles. In both cases, μ_S is found from the net zero strangeness condition. The major difference of the SFO approach is the presence of conservation laws and the corresponding modification of multiplicities due to resonance decays. Thus, we assume that, between two freeze-outs, the system is sufficiently dilute, and, hence, its evolution is governed by the continuous hydrodynamic evolution, which conserves the entropy. Then the equations for the entropy, baryon charge, and isospin projection conservation connecting two freeze-outs are as follows:

$$s_{\text{FO}} V_{\text{FO}} = s_{\text{SFO}} V_{\text{SFO}}, \quad (10)$$

$$n_{\text{FO}}^B V_{\text{FO}} = n_{\text{SFO}}^B V_{\text{SFO}}, \quad (11)$$

$$n_{\text{FO}}^{I3} V_{\text{FO}} = n_{\text{SFO}}^{I3} V_{\text{SFO}}. \quad (12)$$

Getting rid of the effective volumes, we obtain

$$\frac{s}{n^B} \Big|_{\text{FO}} = \frac{s}{n^B} \Big|_{\text{SFO}}, \quad \frac{n^B}{n^{I3}} \Big|_{\text{FO}} = \frac{n^B}{n^{I3}} \Big|_{\text{SFO}}. \quad (13)$$

Therefore, the variables $\mu_{B_{\text{SFO}}}$ and $\mu_{I3_{\text{SFO}}}$ are not free parameters, since they are found from system (13), and only T_{SFO} should be fitted. Thus, for the SFO, the number of independent fitting parameters is 4 for each value of collision energy.

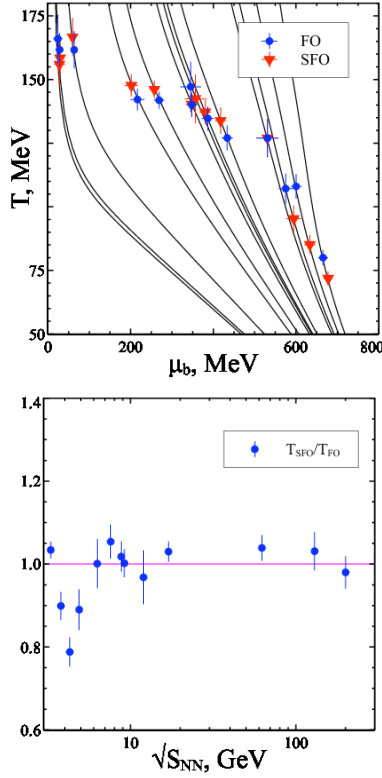


Fig. 1. Parameters of chemical freeze-outs in the model with two freeze-outs. Upper panel: triangles correspond to the SFO, their coordinates are $(\mu_{B_{SFO}}, T_{SFO})$, while circles correspond to the FO, and their coordinates are $(\mu_{B_{FO}}, T_{FO})$. The curves correspond to isentropic trajectories $s/\rho_B = \text{const}$ connecting two freeze-outs. Lower panel: $\sqrt{S_{NN}}$ dependence of the ratio of the SFO temperature to the FO temperature

The number of resonances appeared due to decays are found from

$$\frac{N^{\text{fin}}(X)}{V_{FO}} = \sum_{Y \in FO} BR(Y \rightarrow X) n^{\text{th}}(Y) + \sum_{Y \in SFO} BR(Y \rightarrow X) n^{\text{sth}}(Y) \frac{V_{SFO}}{V_{FO}}. \quad (14)$$

Technically, this is done by multiplying all the thermal concentrations for SFO by $n_{FO}^B/n_{SFO}^B = V_{SFO}/V_{FO}$ and applying the conventional resonance decays.

4. Results

4.1. Data sets and fit procedure

In our choice of the data sets, we basically followed Ref. [2]. Thus, at the AGS energy range of collisions

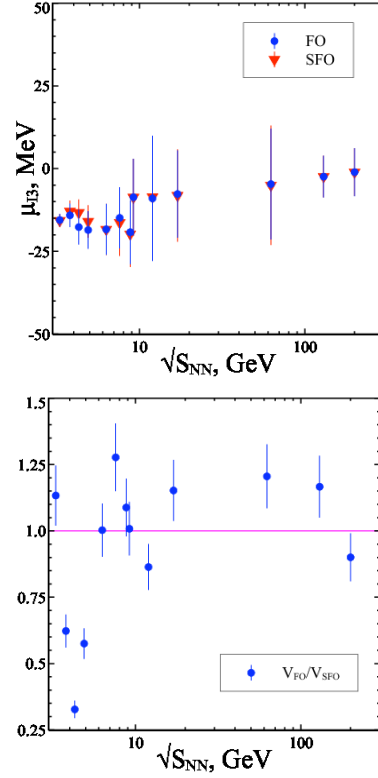


Fig. 2. Upper panel: I_3 chemical potential for the FO (circles) and the SFO (triangles) Lower panel: $\sqrt{S_{NN}}$ dependence of the ratio of the FO volume to the SFO volume

($\sqrt{S_{NN}} = 2.7\text{--}4.9$ GeV), the data are available for the kinetic beam energies from 2 to 10.7 AGeV. For the beam energies 2, 4, 6, and 8 AGeV, there are only a few available data points: the yields for pions [30, 31], for protons [32, 33], for kaons [31] (except for 2 AGeV); for Λ hyperons, the data integrated over 4π are available [34]. For a beam energy of 6 AGeV, there exist the Ξ^- hyperon data integrated over 4π geometry [35]. However, the data for the Λ and Ξ^- hyperons have to be corrected [2], and, instead of the raw experimental data, we used their corrected values of Ref. [2]. For the highest AGS center-of-mass energy $\sqrt{S_{NN}} = 4.9$ GeV (or a beam energy of 10.7 AGeV) in addition to the mentioned data for pions, (anti)protons, and kaons, there exist the data for ϕ meson [36], for Λ hyperon [37], and for $\bar{\Lambda}$ hyperon [38]. Similarly to [5], we analyzed only the NA49 mid-rapidity data [39–44] here, since they are traditionally the most difficult to be described. Because the RHIC high energy data of different collaborations agree with

each other, we present the analysis of the STAR results for $\sqrt{S_{NN}} = 9.2$ GeV [45], $\sqrt{S_{NN}} = 62.4$ GeV [46], $\sqrt{S_{NN}} = 130$ GeV [47–50], and 200 GeV [50–52].

To avoid possible biases, we fit the particle ratios rather than the multiplicities. The best fit criterion is the minimality of $\chi^2 = \sum_i \frac{(r_i^{\text{theor}} - r_i^{\text{exp}})^2}{\sigma_i^2}$, where r_i^{exp} is an experimental value of the i -th particle ratio, r_i^{theor} is our prediction, and σ_i is the total error of the experimental value.

4.2. Fit results

The FO and SFO parameters are connected by the conservation laws (13). Therefore, there is only one fitting parameter at each collision energy for the SFO, namely T_{SFO} , while other parameters are found from system (13). We study two things: the behavior of parameters and which ratios are improved in the SFO approach as compared to the case without SFO. First of all, we found out that, in the SFO case, $\chi^2/\text{dof} = 58.5/55 = 1.06$. At $\sqrt{S_{NN}} = 2.7, 3.3, 3.8, 4.3,$ and 4.9 GeV, the original description obtained within the multicomponent model [5] is very good. Hence, it has not improved significantly. Similar results are found at the highest RHIC energies $\sqrt{S_{NN}} > 62.4$ GeV. From Fig. 1, one can see that, within these two energy domains, the SFO temperatures demonstrate the largest deviations from the FO temperature, although they do not exceed 20%. At intermediate energies, we see a systematic improvement of the description of ratios. Three plots corresponding to the collision energies, at which an improvement after the SFO introduction is the most significant, $\sqrt{S_{NN}} = 6.3, 12,$ and 17 GeV, are shown in Fig. 3. As one can see from Fig. 3 for $\sqrt{S_{NN}} = 6.3, 12,$ and 17 GeV, the SFO approach improves the description of all ratios with more than one σ deviation. For $\sqrt{S_{NN}} = 6.3$ GeV, the SFO greatly improves the $\bar{\Lambda}/\pi^-$ and \bar{p}/p ratios. For $\sqrt{S_{NN}} = 12$ GeV, four ratios of eight ones with more than one σ deviation, namely $K^+/\pi^+, \bar{\Lambda}/\Lambda, \bar{\Lambda}/\pi^-,$ and $\bar{\Xi}^+/\bar{\Xi}^-$ are improved. The SFO approach allows us to significantly improve the fit quality at $\sqrt{S_{NN}} = 17$ GeV. Figure 3 demonstrates that, due to the SFO fit, six of seven problematic ratios for the one-freeze-out fit moved from the region of deviations exceeding σ to the region of deviations being smaller than σ . The most remarkable of them are $\bar{p}/\pi^-, \bar{\Lambda}/\Lambda, \bar{\Xi}^-/\bar{\Xi}^-,$ and $\bar{\Omega}/\Omega$. Thus, the separa-

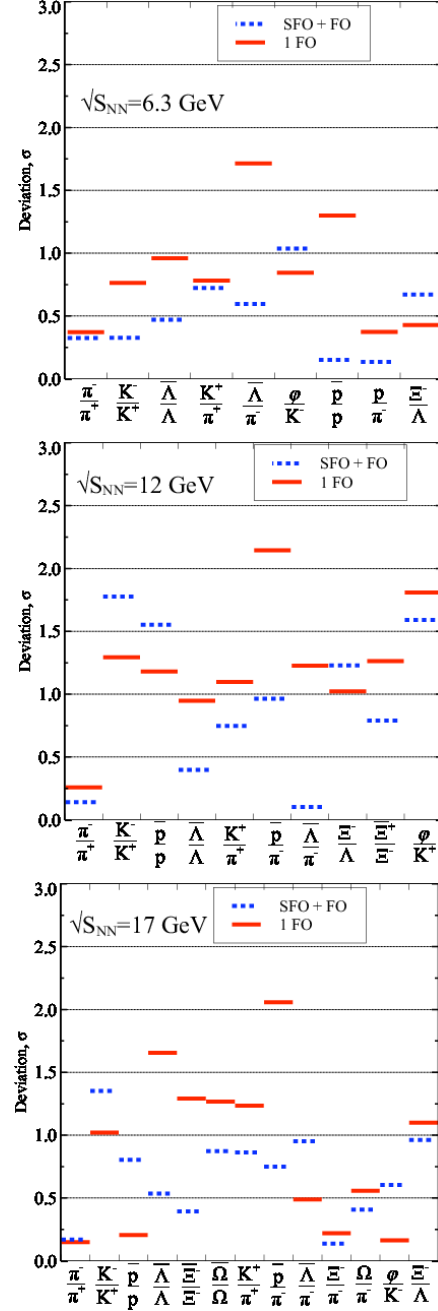


Fig. 3. Relative deviation of the theoretical description of ratios from the experimental value in units of experimental error σ . The symbols on the OX axis demonstrate the particle ratios. The OY axis shows $\frac{|r^{\text{theor}} - r^{\text{exp}}|}{\sigma^{\text{exp}}}$, i.e. the relative deviation modulus for $\sqrt{S_{NN}} = 6.3, 12,$ and 17 GeV. The solid lines correspond to a model with one chemical freeze-out of all hadrons, while the dashed lines correspond to the model with the SFO

tion of the FO and the SFO relaxes the strong connection between the non-strange and strange baryons and allows us not only to nicely describe the ratios of strange antibaryons to the same strange baryons, but also it allows us, for the first time, to successfully reproduce the antiproton to pion ratio.

As we discussed above, it is expected that the SFO occurs earlier, when the system is smaller, and, hence, $V_{\text{SFO}} < V_{\text{FO}}$ or $\frac{V_{\text{FO}}}{V_{\text{SFO}}} > 1$. In the Fig. 2, one can see that this is, indeed, the case for most values of collision energy. But at low energies, our expectation does not come true. One possible formal reason is the same as for the unexpected behavior of $\frac{T_{\text{SFO}}}{T_{\text{FO}}}$ (see Fig. 1): in this energy range, the number of data points is just slightly larger than the number of fitting parameters, and, because of that, the fit quality at low energies of collisions is very good without assumption of two freeze-outs. There might be also a physical reason for such a behavior. Namely, the freeze-out at low collision energies occurs at large baryonic densities, which may essentially affect the in-medium cross-sections of the reactions with strangeness exchange due to the additional attraction. Therefore, such reactions do not freeze-out earlier than other reactions.

Finally, we would like to suggest a generalization of the double freeze-out HRGM that will be able to ultimately improve the description of multiplicities. The first step is to identify the hadronic reactions that freeze-out noticeably earlier or later than most of the others. This should be done separately for each collision energy, since the reaction cross-sections, particle concentrations, and fireball expansion rate are different at different energies. Such reactions may be identified, by using system (1) or by running the transport model code and by counting for the reaction rates versus the time. If such reactions exist, then their separate freeze-out should be considered. It is clear that the conservation laws between the freeze-outs may be different, by depending on which reactions are switched-off. For instance, if all reactions with the Ω hyperon are frozen, then the conservation law of the number of Ω hyperons should be introduced. Probably, the charmed particles are good candidates for the separate freeze-out.

5. Conclusions

We have thoroughly discussed the assumption that, in heavy ion collisions, the strangeness exchange reac-

tions may freeze-out earlier. Using such assumption, we have constructed a modification of the HRGM with two freeze-outs, which is connected with the conservation laws. One freeze-out corresponds to all strange particles, and another freeze-out is for all non-strange ones. The conservation laws allow us to get just one additional fitting parameter for each collision energy, as compared to the HRGM with a simultaneous chemical freeze-out of all hadrons. We have shown that such a model describes 111 independent hadron ratios measured at $\sqrt{S_{NN}} = 2.7\text{--}200$ GeV even better than the most elaborate version of the HRGM with a single freeze-out ($\chi^2/\text{dof} = 1.06$ for the model with two freeze-outs versus 1.16 for one freeze-out).

We suggest to go even further: for each collision energy, to separately identify the processes, which freeze-out at considerably different times than all the others and to construct a corresponding HRGM with two freeze-outs. The identification of such reactions can be done, by using the transport models.

The authors are thankful to P. Huovinen for fruitful discussions. D.R.O. acknowledges the funding of the Helmholtz Young Investigator Group VH-NG-822 from the Helmholtz Association and GSI, and thanks HGS-HIRe for a support. A.I.I. and K.A.B. acknowledge a support of the Fundamental Research State Fund of Ukraine, Project No. F58/04. K.A.B. acknowledges a partial support provided by the Helmholtz International Center for FAIR within the framework of the LOEWE program launched by the State of Hesse.

1. P. Braun-Munzinger, K. Redlich, and J. Stachel, in: *Quark Gluon Plasma*, edited by R.C. Hwa et al., World Scientific, Singapore, 2003, p. 491.
2. A. Andronic, P. Braun-Munzinger, and J. Stachel, Nucl. Phys. A **772**, 167 (2006) and references therein.
3. F. Becattini, J. Phys. G **23**, 1933 (1997).
4. F. Becattini, J. Manninen, and M. Gazdzicki, Phys. Rev. C **73**, 044905 (2006).
5. K.A. Bugaev, D.R. Oliinychenko, A.S. Sorin, and G.M. Zinovjev, Eur. Phys. J. A **49**, 30–1–8 (2013) and references therein.
6. B. Friman et al. (Eds.), *The CBM physics book*, Lect. Notes Phys. **814**, Springer, 2010.
7. J. Rafelski, Phys. Lett. B **62**, 333 (1991).
8. P. Braun-Munzinger, D. Magestro, K. Redlich, and J. Stachel, Phys. Lett. B **518**, 41 (2001).
9. K.A. Bugaev, D.R. Oliinychenko, J. Cleymans, A.I. Ivanytskyi, I.N. Mishustin, E.G. Nikonov, and V.V. Sagun, Europhys. Lett. **104**, 22002 (2013).

10. K.A. Bugaev, J. Phys. G **28**, 1981 (2002).
11. M.I. Gorenstein, K.A. Bugaev, and M. Gazdzicki, Phys. Rev. Lett. **88**, 132301 (2002).
12. K.A. Bugaev, M. Gazdzicki, and M.I. Gorenstein, Phys. Lett. B **544**, 127 (2002).
13. E. Fermi, Prog. Theor. Phys. **5**, 570 (1950).
14. L.D. Landau, Izv. Akad. Nauk. SSSR, Ser. Fiz. **17**, 51 (1953).
15. J. Stachel *et al.*, arXiv: 1311.4662 [nucl-th].
16. K. Redlich *et al.*, J. Phys. G. **36**, 064021 (2009).
17. M. Gyulassy and X.N. Wang, Nucl. Phys. B **420**, 583 (1994).
18. X.N. Wang, M. Gyulassy, and M. Plümer, Phys. Rev. D **51**, 3436 (1995).
19. R. Baier, Yu.L. Dokshitzer, S. Peigne, and D. Schiff, Phys. Lett. B **345**, 277 (1995).
20. K.A. Bugaev *et al.*, NICA White Paper, Draft 9.01, Contribution 4.21, published on 6 of June, 2013; <http://theor.jinr.ru/twiki/pub/NICA/NICAWHITEPAPER>.
21. S. Chatterjee, R.M. Godbole, and S. Gupta, Phys. Lett. B **727**, 554 (2013).
22. D.R. Oliinychenko, K.A. Bugaev, and A.S. Sorin, Ukr. J. Phys. **58**, 211 (2013).
23. K.A. Bugaev, M.I. Gorenstein, H. Stöcker, and W. Greiner, Phys. Lett. B **485**, 121 (2000).
24. G. Zeeb, K.A. Bugaev, P.T. Reuter, and H. Stöcker, Ukr. J. Phys. **53**, 279 (2008).
25. K.A. Bugaev, Nucl. Phys. A **807**, 251 (2008); arXiv:nucl-th/0611102.
26. K.A. Bugaev, D.R. Oliinychenko, and A.S. Sorin, Ukr. J. Phys. **58**, 939 (2013).
27. K.A. Bugaev, A.I. Ivanytskyi, D.R. Oliinychenko, E.G. Nikonov, V.V. Sagun, and G.M. Zinovjev, arXiv: 1312.4367 [hep-ph].
28. K.A. Bugaev, D.R. Oliinychenko, V.V. Sagun, A.I. Ivanytskyi, J. Cleymans, E.G. Nikonov, and G.M. Zinovjev, arXiv: 1312.5149 [hep-ph].
29. S. Wheaton, J. Cleymans, and M. Hauer, Comput. Phys. Commun. **180**, 84 (2009).
30. J.L. Klay *et al.*, Phys. Rev. C **68**, 054905 (2003).
31. L. Ahle *et al.*, Phys. Lett. B **476**, 1 (2000).
32. B.B. Back *et al.*, Phys. Rev. Lett. **86**, 1970 (2001).
33. J.L. Klay *et al.*, Phys. Rev. Lett. **88**, 102301 (2002).
34. C. Pinkenburg *et al.*, Nucl. Phys. A **698**, 495c (2002).
35. P. Chung *et al.*, Phys. Rev. Lett. **91**, 202301 (2003).
36. B.B. Back *et al.*, Phys. Rev. C **69**, 054901 (2004).
37. S. Albergo *et al.*, Phys. Rev. Lett. **88**, 062301 (2002).
38. B.B. Back *et al.*, Phys. Rev. Lett. **87**, 242301 (2001).
39. S.V. Afanasiev *et al.*, Phys. Rev. C **66**, 054902 (2002).
40. S.V. Afanasiev *et al.*, Phys. Rev. C **69**, 024902 (2004).
41. T. Anticic *et al.*, Phys. Rev. Lett. **93**, 022302 (2004).
42. S.V. Afanasiev *et al.*, Phys. Lett. B **538**, 275 (2002).
43. C. Alt *et al.*, Phys. Rev. Lett. **94**, 192301 (2005).
44. S.V. Afanasiev *et al.*, Phys. Lett. B **491**, 59 (2000).
45. B. Abelev *et al.*, Phys. Rev. C **81**, 024911 (2010).
46. B. Abelev *et al.*, Phys. Rev. C **79**, 034909 (2009).
47. J. Adams *et al.*, Phys. Rev. Lett. **92**, 182301 (2004).
48. J. Adams *et al.*, Phys. Lett. B **567**, 167 (2003).
49. C. Adler *et al.*, Phys. Rev. C **65**, 041901(R) (2002).
50. J. Adams *et al.*, Phys. Rev. Lett. **92**, 112301 (2004).
51. J. Adams *et al.*, Phys. Lett. B **612**, (2005) 181.
52. A. Billmeier *et al.*, J. Phys. G **30**, S363 (2004).

Received 11.03.14

*Д.Р. Олійниченко,**В.В. Сагун, О.І. Іваницький, К.О. Бугаєв*

ВІДОКРЕМЛЕНИЙ ХІМІЧНИЙ ФРІЗАУТ ДИВНИХ ЧАСТИНОК ІЗ ЗАКОНАМИ ЗБЕРЕЖЕННЯ

Резюме

Розглянуто модель адронного резонансного газу із двома фрізаутами, що пов'язані між собою законами збереження. Наведено аргументи на користь того, що хімічний фрізаут дивних адронів має відбуватися раніше, ніж хімічний фрізаут недивних адронів. За допомогою представленої моделі виконано високоякісний фіт адронних множинностей, виміряних у зіткненнях важких іонів при енергіях зіткнення в системі центра мас від 2,7 до 200 GeV. Ґрунтуючись на успіху даного підходу, нами запропоновано спосіб радикального вдосконалення моделі адронного резонансного газу. Для цього ми пропонуємо визначати адронні реакції, які припиняються раніше або пізніше, ніж більшість інших реакцій (для різних енергій зіткнень вони можуть бути різними), та розглядати для цих реакцій відокремлені фрізаути.